Dalton Transactions

ROYAL SOCIETY OF CHEMISTRY

COMMUNICATION

View Article Online
View Journal | View Issue

Cite this: *Dalton Trans.*, 2022, **51**, 15239

Received 13th July 2022,
Accepted 30th September 2022

DOI: 10.1039/d2dt02281h

rsc.li/dalton

Selective recognition and extraction of arsenate by a urea-functionalized tripodal receptor from competitive aqueous media†

Sandeep Kumar Dey, *[a,b] Beatriz Gil-Hernández, [c] Vivekanand V. Gobre,[d] Dennis Woschko, [e] Sarvesh S. Harmalkar,[d] Firdaus Rahaman Gayen,[a,b] Biswajit Saha, [a,b] Rajib Lochan Goswamee[a,b] and Christoph Janiak [e]

A second-generation hydrogen bond donor (HBD) anion receptor with an inner amide cavity and an outer urea cavity can selectively and efficiently extract arsenate (AsO_4^{3-}) from water in the presence of competitive oxoanions and halides. The X-ray structure showed encapsulation of AsO_4^{3-} in a π-stacked dimeric capsular assembly of the receptor, the first crystallography-based example of pentavalent AsO_4^{3-} trianion recognition by a HBD receptor.

Introduction

Ground water aquifers have long been the primary source of drinking water to mankind. However, many of these aquifers are contaminated with naturally occurring toxic ions leaching out from the underlying rocks and soil that surround the aquifers. Arsenic contamination of ground water is a global problem arising from naturally occurring arsenic oxide (As_2O_3), which reacts with water to form hydrogenarsenite ($H_2AsO_3^- \rightleftarrows HAsO_3^{2-}$) and eventually gets oxidized to hydrogenarsenate ($H_2AsO_4^- \rightleftarrows HAsO_4^{2-}$).[1] Millions of people in India, Bangladesh, South-East Asia and South America, are consuming arsenic-contaminated water every day.[2] Furthermore, arsenic has also entered the human food chain due to excessive ground water irrigation in arsenic-contaminated regions and the extensive use of arsenical pesticides in agriculture. Prolonged exposure to inorganic arsenic from drinking water and food increases the risks of developing cancer and other health issues including skin lesions and abdominal ailments among others.[3] In spite of the significant advancement made in water-purification technologies, people from many countries struggle to have safe drinking water, mainly due to poverty and partly due to a lack of awareness and government initiatives.[4] We believe that, while water purification remains the first line of defense to counter arsenic poisoning (arsenicosis), efforts should also be made to develop highly effective chelation therapeutic agents for arsenicosis with fewer or no side-effects, similar to iron chelation therapy by synthetic siderophores.[5]

HBD anion receptors have been widely studied for the selective recognition of anions (halides and oxoanions), largely in the past two decades.[6] However, there are very few examples of HBD anion receptors which can selectively bind an arsenate species ($H_2AsO_4^-$, $HAsO_4^{2-}$, AsO_4^{3-}) in solution.[7] In contrast, phosphate and sulfate selective HBD anion receptors are numerous in the literature.[8] Due to the presence of several competitive anions (F^-, Cl^-, NO_3^-, CO_3^{2-}, SO_4^{2-} and HPO_4^{2-}) in the natural water sources and the high hydration enthalpies of arsenates, selective arsenate recognition and extraction by synthetic receptors is a highly challenging task that it would be exciting to achieve.

Thus, the development of HBD anion receptors having higher binding affinity for arsenate in comparison with halides and other competitive oxoanions present in water is of significant importance. Urea-based *N*-bridged tripodal scaffolds are generally considered as ideal receptors for the encapsulation of oxoanions, and some of these receptors are known for the selective recognition of sulfate and phosphate.[8,9]

Herein, we report the selective recognition and extraction of arsenate (AsO_4^{3-}) from water by a urea-functionalized tripodal receptor **L** (Scheme 1) in the presence of competitive anions (OH^-, F^-, Cl^-, CH_3COO^-, NO_3^-, CO_3^{2-}, SO_4^{2-} and HPO_4^{2-}).

[a]*Materials Science and Technology Division, CSIR-North East Institute of Science and Technology, Jorhat, Assam, 785006, India. E-mail: sandeep@neist.res.in*
[b]*Academy of Scientific and Innovative Research (AcSIR), Ghaziabad-201002, Uttar Pradesh, India*
[c]*Departmento de Química, Facultad de Ciencias, Sección Química, Universidad de La Laguna, 38206 La Laguna, Tenerife, Spain. E-mail: beagher@ull.es*
[d]*School of Chemical Sciences, Goa University, Taleigao Plateau, Goa 403206, India. E-mail: vvgobre@unigoa.ac.in*
[e]*Institute of Inorganic and Structural Chemistry, Heinrich-Heine University, Düsseldorf, 40225, Germany. E-mail: janiak@uni.duesseldorf.de*

† Electronic supplementary information (ESI) available: Synthesis and characterization of the receptor and oxoanion complexes, NMR spectra, HR-MS, XRD details and DFT calculation table. CCDC 2172773. For ESI and crystallographic data in CIF or other electronic format see DOI: https://doi.org/10.1039/d2dt02281h

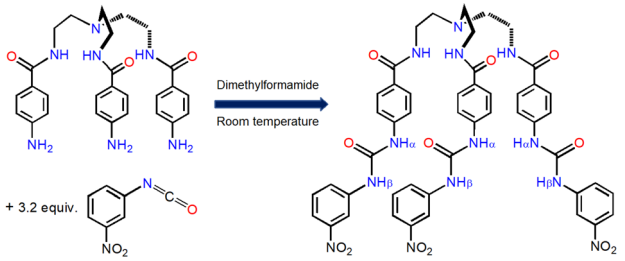

Scheme 1 Synthesis of hydrogen bond donor tripodal receptor **L** (yield 62%).

Single crystal X-ray structural analysis showed the encapsulation of an arsenate in a π-stacked rigidified dimeric capsular assembly of the receptor by multiple charge-assisted hydrogen bonds. Density functional theory (DFT)-based binding energy calculations showed the highest binding affinity of **L** for AsO_4^{3-} followed by PO_4^{3-} and CO_3^{2-} in the energy-optimized receptor–oxoanion complexes.

Results and discussion

In our effort to achieve the selective recognition of an oxoanion by encapsulation within a HBD organic scaffold, we have synthesized a second-generation tripodal receptor **L** (Scheme 1) having an inner amide cavity and an outer urea cavity. The solution-state anion binding properties of **L** were investigated using ^{1}H-NMR spectroscopy in DMSO-D_6 (99.9% D atom) at 298 K. In a typical qualitative ^{1}H-NMR experiment, 15 mg of **L** was dissolved in DMSO-D_6 (0.6 mL) and 1–2 equivalents of a quaternary ammonium (Et_4N^+ or n-Bu_4N^+) salt were added to the solution.

The ^{1}H-NMR spectrum of **L** (DMSO-D_6) showed the amide –NH signal at 8.2 ppm and the urea –NH protons appeared at 9.0 and 9.2 ppm for $-NH_\alpha$ and $-NH_\beta$ respectively (Fig. 1a). ^{1}H-NMR studies revealed the participation of the urea $-NH_{\alpha,\beta}$ protons of **L** in strong hydrogen bonding with F^-, Cl^-, $H_2PO_4^-$ and HSO_4^-. The addition of (n-Bu_4N^+)$H_2PO_4^-$ and (n-Bu_4N^+)HSO_4^- to individual solutions of **L** (DMSO-D_6) resulted in a significant downfield shift of the urea $-NH_{\alpha,\beta}$ signals ($\Delta\delta$ = 1.10–1.25 ppm) with concomitant peak broadening (Fig. 1b and c), suggesting strong hydrogen bonding between the receptor and the tetrahedral oxoanion. The addition of (n-Bu_4N^+)CH_3COO^- also showed a downfield shift of the urea $-NH_{\alpha,\beta}$ signals ($\Delta\delta$ = 0.50–0.55 ppm) but without any concomitant broadening, and no notable changes were observed in the amide –NH and aromatic –CH signals (Fig. 1d). However, the addition of (n-Bu_4N^+)NO_3^- and (n-Bu_4N^+)ClO_4^- did not induce any observable spectral changes with respect to **L**, indicating negligible interaction of the urea $-NH_{\alpha,\beta}$ protons with nitrate and perchlorate ions (Fig. 1e and S22, ESI†). Among halides, the addition of (Et_4N^+)F^- showed the complete disappearance of the urea $-NH_{\alpha,\beta}$ signals, indicating hydrogen bond-induced rapid dynamic effects which lead to significant broadening so

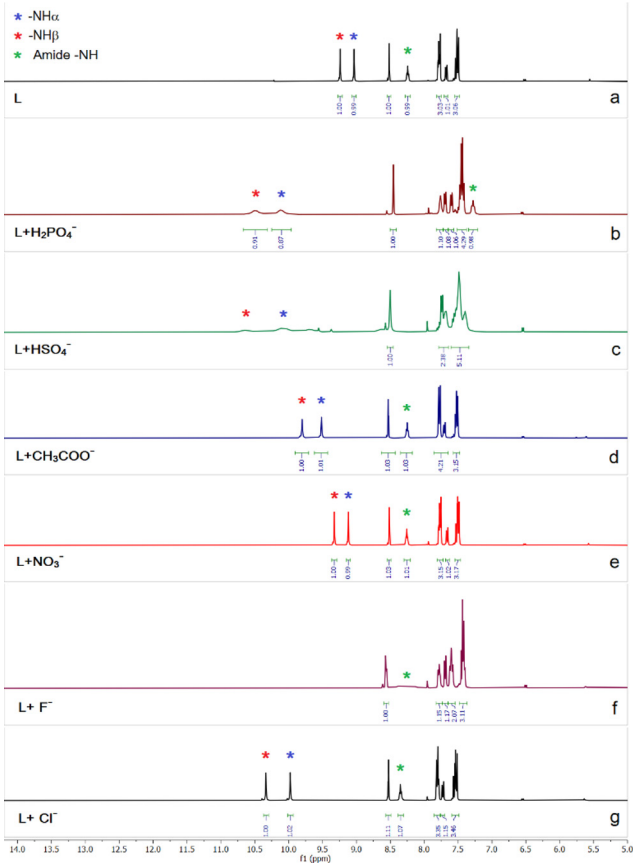

Fig. 1 Aromatic region of the ^{1}H-NMR spectra of (a) receptor **L**, and in the presence of quaternary ammonium salts of (b) dihydrogenphosphate, (c) hydrogensulfate, (d) acetate, (e) nitrate, (f) fluoride and (g) chloride in DMSO-D_6 (full spectra are provided in the ESI,† Fig. S1 and S15–S22).

that the signals disappear in the base line (Fig. 1f). In contrast, the addition of (Et_4N^+)Cl^- showed a downfield shift of the urea $-NH_{\alpha,\beta}$ signals ($\Delta\delta$ = 0.95–1.10 ppm), but without any observable change in the aromatic –CH signals (Fig. 1g). Similar to (n-Bu_4N^+)NO_3^- and (n-Bu_4N^+)ClO_4^-, the addition of (Et_4N^+)Br^- did not show any observable spectral changes of **L** (Fig. S21, ESI†).

Based on the receptor–anion interactions observed in the ^{1}H-NMR experiments, we have carried out liquid–liquid extraction of three tetrahedral oxoanions (phosphate, sulfate and arsenate) by **L** in the presence of (n-Bu_4N^+)OH^- to obtain the hydrogen-bonded receptor–oxoanion complexes from the organic phase. In a typical liquid–liquid extraction experiment, **L** (200 mg) was dissolved in dichloromethane (DCM, 20 mL) in the presence of three equivalents of (n-Bu_4N^+)OH^- and an aqueous solution of an oxoanion (1 equiv. of Na_2HPO_4, Na_2HAsO_4 or Na_2SO_4, dissolved in 20 mL of water) was added to the DCM solution and stirred for half an hour. The hydrogen-bonded receptor–oxoanion complex was obtained from the separated organic phase as a yellow crystalline powder and characterized using NMR (DMSO-D_6) and HR-MS (CH_3CN) in each case. Extraction experiments have also been performed

separately in the presence of $(n\text{-}Bu_4N^+)F^-$ to obtain the respective receptor–oxoanion complexes of phosphate, sulfate and arsenate, indicating that receptor **L** has a higher binding affinity for these oxoanions as compared to basic fluoride and hydroxide.

The ^{1}H-NMR spectra of arsenate and phosphate complexes were observed to be similar where the urea –NH signals appeared to be downfield shifted at 11.8 ($\Delta\delta$ = 2.75 ppm) and 12.9 ($\Delta\delta$ = 3.65 ppm) ppm for $-NH_\alpha$ and $-NH_\beta$ respectively (Fig. S4 and S7, ESI†). Due to strong hydrogen bonding interactions of the urea $-NH_{\alpha,\beta}$ groups with the arsenate/phosphate, the electronic environment of the adjacent aromatic rings was affected and therefore broadening and changes in peak positions were also observed for the aromatic –CH signals (Fig. 2a–c). Integration of the ^{1}H-NMR signals suggested that there are three tetrabutylammonium ($n\text{-}Bu_4N^+$) cations present in the arsenate and phosphate complexes, and AsO_4^{3-}/PO_4^{3-} is coordinated to two receptor molecules (Fig. S4 and S7, ESI†). The formation of the 2 : 1 receptor–oxoanion complex was further confirmed by single crystal X-ray diffraction analysis of $[(n\text{-}Bu_4N)_3(2\mathbf{L}\cdot AsO_4)]$ and HR-MS (Fig. S6 and S10, ESI†). The ^{31}P-NMR spectrum of the phosphate complex showed a signal at 8.1 ppm for the hydrogen-bonded PO_4^{3-} ion (Fig. S8, ESI†). The ^{1}H-NMR spectrum of the sulfate complex also showed a downfield shift of the urea $-NH_\alpha$ and $-NH_\beta$ signals appearing at 10.0 ($\Delta\delta$ = 1.0 ppm) and 10.5 ($\Delta\delta$ = 1.25 ppm) ppm respectively, with observable changes in the aromatic –CH signals (Fig. 2d and S11, ESI†).

Single crystals of the arsenate complex suitable for X-ray diffraction analysis were obtained from a dimethyl sulfoxide (DMSO) solution of the extracted compound under ambient conditions. The crystal structure of the hydrogen-bonded arsenate complex showed the encapsulation of the tetrahedral oxoanion in a π-stacked dimeric capsular assembly of receptor

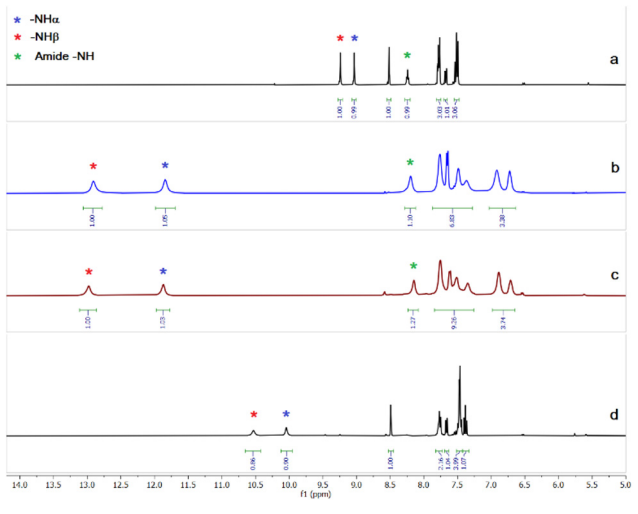

Fig. 2 Aromatic region of the ^{1}H-NMR spectra of (a) receptor **L**, (b) crystals of the arsenate complex $[(n\text{-}Bu_4N)_3(2\mathbf{L}\cdot AsO_4)]$, (c) crystals of the phosphate complex $[(n\text{-}Bu_4N)_3(2\mathbf{L}\cdot PO_4)]$, and (d) crystals of the sulfate complex $[(n\text{-}Bu_4N)_2(2\mathbf{L}\cdot SO_4)]$ in DMSO-D_6 (full spectra are provided in the ESI,† Fig. S1, S4, S7 and S11).

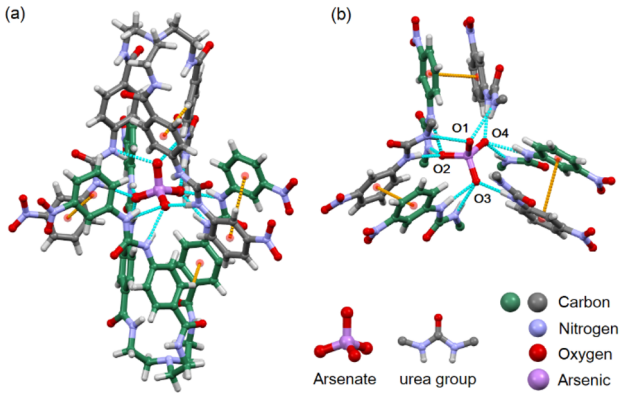

Fig. 3 X-ray crystal structure of the arsenate complex $[(n\text{-}Bu_4N)_3(2\mathbf{L}\cdot AsO_4)]$ showing (a) encapsulation of AsO_4^{3-} by two symmetry-independent receptor molecules (shown in different colours) *via* eleven N–H···O hydrogen bonds (counter cations are not shown), and (b) hydrogen bond interactions of the encapsulated AsO_4^{3-} with the six urea groups of the dimeric assembly of **L** engaged in π–π interactions between the nitrophenyl rings.

L, $[(n\text{-}Bu_4N)_3(2\mathbf{L}\cdot AsO_4)]$ (Fig. 3a and S61, ESI†). Structural elucidation revealed that the complex $[(n\text{-}Bu_4N)_3(2\mathbf{L}\cdot AsO_4)]$‡ crystallized in the triclinic $P\bar{1}$ space group (Z = 2), where the encapsulated AsO_4^{3-} is hydrogen bonded to the six urea groups of two symmetry-independent receptor molecules by at least eleven N–H···O hydrogen bonds (Fig. 3). Three arsenate oxygen atoms (O2, O3 and O4) accept three hydrogen bonds each and another arsenate oxygen (O1) accepts two hydrogen bonds from the urea groups of two receptor molecules assembled by the π–π interactions of the nitrophenyl rings (Fig. 3b). The N–H···O hydrogen bond donor–acceptor distances range between 2.70 and 2.88 Å (Table S2, ESI†), and the distances between the centroids of the peripheral aromatic rings involved in π–π interactions are 3.75–4.12 Å.

The powder X-ray diffraction (PXRD) patterns of the crystals of the arsenate complex obtained from a DMSO solution closely resemble the simulated PXRD patterns of the single crystal X-ray structure of $[(n\text{-}Bu_4N)_3(2\mathbf{L}\cdot AsO_4)]$, suggesting the exclusive crystallization of one type of host–guest complex (Fig. S38 and S39, ESI†). Single crystals of the phosphate complex could also be obtained from a DMSO solution of the extracted compound under ambient conditions. However, the crystal structure could not be solved due to the poor diffraction data quality. The ^{1}H-NMR and UV-vis spectra of the crystals of the phosphate complex were observed to be similar to those of the arsenate complex (Fig. 2 and S41, ESI†). However, the PXRD patterns of the crystals of the phosphate complex were observed to be different from the simulated PXRD patterns of $[(n\text{-}Bu_4N)_3(2\mathbf{L}\cdot AsO_4)]$, suggesting solid-state structural dissimilarities to the arsenate complex (Fig. S40, ESI†). 2D-NOESY NMR experiments (DMSO-D_6) have also been performed to validate the encapsulation of AsO_4^{3-}/PO_4^{3-} by **L**. The free receptor molecule showed intense NOESY signals (contours) in the aromatic region of the 2D spectrum, indicating strong interactions between the urea protons ($-NH_\alpha$ and $-NH_\beta$) and

among the aromatic –CH protons (Fig. S32 and S33, ESI†). However, the crystals of the AsO_4^{3-} and PO_4^{3-} complexes showed considerably weak NOESY signals in the aromatic region, possibly due to the strong interactions of the urea groups with the encapsulated oxoanion (Fig. S34–S37, ESI†).[10]

In an attempt to evaluate the association constants of receptor–oxoanion binding, we have carried out ^{1}H-NMR titration experiments of receptor **L** in the presence of Na_2HAsO_4 and Na_2HPO_4 in DMSO-D_6/D_2O (9 : 1, v/v) solution.[11] The ^{1}H-NMR spectrum of **L** in DMSO-D_6/D_2O (9 : 1, v/v) showed the disappearance of the urea –$NH_{\alpha,\beta}$ signals (Fig. S42, ESI†), unlike the ^{1}H-NMR spectrum of **L** in neat DMSO-D_6 (Fig. S1, ESI†). Thus, the gradual downfield shift of the urea –$NH_{\alpha,\beta}$ signals could not be followed upon addition of aliquots of Na_2HAsO_4 or Na_2HPO_4 (in DMSO-D_6/D_2O) to determine the association constants of these oxoanions with **L** (Fig. S43–S46, ESI†).

However, the ^{31}P NMR signals of both the phosphate complex (crystals) and 1 : 1 receptor–Na_2HPO_4 solution in DMSO-D_6/D_2O (9 : 1, v/v) appeared at 8.2 ppm, suggesting the presence of the same phosphate species in both the solutions (Fig. S47 and S48, ESI†). In contrast, the ^{31}P NMR signal of (n-Bu_4N^+)$H_2PO_4^-$ was observed at 0.08 ppm in DMSO-D_6/D_2O (Fig. S49, ESI†).[12] Thus, a large downfield shift of 8.1 ppm was observed for the hydrogen-bonded phosphate in [(n-Bu_4N)$_3$(2**L**·PO_4)] with respect to the ^{31}P NMR of the free dihydrogenphosphate anion (Fig. S50, ESI†).[13]

Unlike the ^{1}H-NMR spectrum of **L** in DMSO-D_6/D_2O (9 : 1, v/v), the spectrum of **L** in DMSO-D_6/H_2O (9 : 1, v/v) solution showed the appearance of urea –$NH_{\alpha,\beta}$ signals (Fig. S51, ESI†). Incremental addition of an aqueous solution of Na_2HAsO_4 to a DMSO-D_6/H_2O (9 : 1, v/v) solution of **L** showed the appearance of more than two urea –NH signals (broad), indicating the presence of multiple hydrogen-bonded species (the possible coexistence of $[2\mathbf{L}\cdot HAsO_4]^{2-}$ and $[2\mathbf{L}\cdot AsO_4]^{3-}$ complexes) in the solution, and thus the association constant could not be determined from the ^{1}H-NMR titration experiment (Fig. S52–S54, ESI†).[8d] However, the receptor–arsenate complex obtained from the extraction experiment was observed to be of type [(n-Bu_4N)$_3$(2**L**·AsO_4)] only, as proved by ^{1}H-NMR, HR-MS, single-crystal XRD and powder XRD analyses of the crystals.

Since the association constants of receptor–oxoanion binding could not be evaluated from ^{1}H-NMR titration experiments, we carried out binding energy (BE) calculations based on density functional theory (DFT). BE calculations were performed to understand the binding affinity of **L** for various oxoanions (X = AsO_4^{3-}, PO_4^{3-}, SO_4^{2-}, CO_3^{2-} and NO_3^-), BE = (E_L + E_X) − E_{LX} in Hartree (1 Hartree = 2625.5 kJ mol^{-1}). Energy optimization of the receptor–oxoanion complexes was carried out using hybrid-DFT at the B97D/6-31G** level of theory (Fig. S55–S59, ESI†).[14] DFT calculations revealed that the binding affinity of **L** for AsO_4^{3-} is the highest followed by PO_4^{3-}, CO_3^{2-}, SO_4^{2-} and NO_3^-. The BE of **L** for AsO_4^{3-} (−3583.9 kJ mol^{-1}) is higher than the BE for PO_4^{3-} (−3515.1 kJ mol^{-1}), and they are more than double the BE for SO_4^{2-} (−1419.9 kJ mol^{-1}) and CO_3^{2-} (−1662.2 kJ mol^{-1}), and more than four times the BE for NO_3^- (−781.5 kJ mol^{-1}) (Table S1, ESI†).

The highest binding affinity of **L** for AsO_4^{3-} encouraged us to perform liquid–liquid extraction of AsO_4^{3-} from water in the presence of competitive anions (F^-, Cl^-, CH_3COO^-, CO_3^{2-}, SO_4^{2-}, and NO_3^-). In a typical competitive extraction experiment, **L** (200 mg) was dissolved in dichloromethane (20 mL DCM) in the presence of three equivalents of (n-Bu_4N^+)OH^- and an aqueous solution mixture of hydrogenarsenate and two competitive anions (1 equivalent of sodium salts of (i) $HAsO_4^{2-}$, F^- and Cl^- (pH 8.8), (ii) $HAsO_4^{2-}$, CH_3COO^- and CO_3^{2-} (pH 10.6), and (iii) $HAsO_4^{2-}$, SO_4^{2-} and NO_3^- (pH 8.9), dissolved in 20 mL of water) was added to the DCM solution and stirred for half an hour. The yellow crystalline solid obtained from the DCM solution was characterized by NMR and HR-MS analyses. The ^{1}H-NMR spectra of the extracted compounds closely resemble the spectrum of the [(n-Bu_4N)$_3$(2**L**·AsO_4)] crystals in each case, suggesting the selective extraction of arsenate in competitive media (Fig. 4 and Fig. S23–S25, ESI†). Notably, the chemical shift of the urea –NH signals (–NH_α at 11.80 and –NH_β at 12.90 ppm), and the integral values of the aromatic –CH peaks and tetrabutylammonium peaks are all observed to be similar in the spectra obtained. It has to be noted that the yield of the arsenate complexes was calculated to be 90–92% (relative to **L**) in all three cases of the competitive extraction experiments. It is remarkable to note that AsO_4^{3-} extraction from water occurs so efficiently by the exchange of OH^- ions with deprotonated $HAsO_4^{2-}$ between the two immiscible phases, representing the very high affinity of the urea-based receptor **L** for AsO_4^{3-}.

Furthermore, extraction experiments were also carried out with aqueous solutions of Na_2HAsO_4 adjusted to different pH

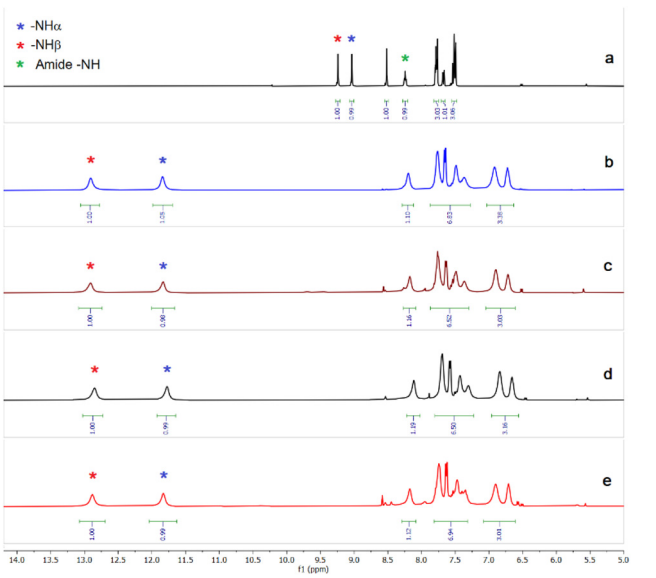

Fig. 4 Aromatic region of the ^{1}H-NMR spectra of (a) receptor **L**, (b) crystals of arsenate complex [(n-Bu_4N)$_3$(2**L**·AsO_4)], (c) arsenate complex extracted in the presence of fluoride and chloride, (d) arsenate complex extracted in the presence of carbonate and acetate, and (e) arsenate complex extracted in the presence of sulfate and nitrate (full spectra are provided in the ESI,† Fig. S1, S4 and S23–S25).

values (5.5, 7.4, 9.5 and 11) with Na_2CO_3 and CH_3COOH. The pH of the aqueous solution affects the speciation of the species distribution of arsenate given by the equilibria $H_3AsO_4 \rightleftarrows H_2AsO_4^- + H^+$ ($pK_{a1} = 2.3$), $H_2AsO_4^- \rightleftarrows HAsO_4^{2-} + H^+$ ($pK_{a2} = 6.8$), and $HAsO_4^{2-} \rightleftarrows AsO_4^{3-} + H^+$ ($pK_{a3} = 11.6$).[7c,d] An aqueous solution of Na_2HAsO_4 (18.5 mg in 20 mL water, ~1% solution) has a pH value of 8.8 (Fig. S65, ESI†), and it has already been discussed that arsenate can be efficiently extracted by **L** in DCM solution in the presence of three equivalents of $(n\text{-}Bu_4N^+)OH^-$ by anion exchange between the two immiscible phases. Similarly, the efficient extraction of arsenate by **L** was also achieved from the aqueous solutions of Na_2HAsO_4 at basic pH values of 7.4, 9.5 and 11 with a 90% yield of the arsenate complex $[(n\text{-}Bu_4N)_3(2\mathbf{L}\cdot AsO_4)]$ (Fig. S60–S62, ESI†). However, arsenate extraction by **L** could not be achieved from an aqueous solution of Na_2HAsO_4 at acidic pH 5.5. The HR-MS and ^{1}H-NMR spectra of the extracted compound obtained under acidic conditions (Fig. S63 and S64, ESI†) do not match the spectra of the arsenate complexes obtained under basic conditions (pH 7.4, 8.8, 9.5 and 11) in liquid–liquid extraction experiments.

Finally, in order to validate the selective extraction of arsenate over phosphate, an extraction experiment was performed using an aqueous solution mixture of one equiv. of Na_2HAsO_4 and Na_2HPO_4 (pH 8.8). ^{31}P-NMR spectroscopy confirmed the absence of phosphate in the extracted complex (signal at 8.1 ppm not observed), and HR-MS analysis validated the selective extraction of arsenate in the presence of phosphate (Fig. S26 and S27, ESI†). However, phosphate could easily be extracted by **L** in the presence of halides (F^- and Cl^-) and oxoanions (SO_4^{2-} and NO_3^-) from aqueous media (Fig. S28–S31, ESI†). AsO_4^{3-} and PO_4^{3-} are tetrahedral oxoanions of the same group and thus have close similarities in terms of their ionic charge, thermodynamic radii, pK_a values and hydration energy.[15] Therefore, the liquid–liquid extraction of arsenate in the presence of highly competitive phosphate and other anions by **L** is a significant accomplishment.

Since all the arsenate extraction experiments were carried out in the presence of three equivalents of $(n\text{-}Bu_4N^+)OH^-$ or $(n\text{-}Bu_4N^+)F^-$, it is necessary to assess the interaction of receptor **L** with hydroxide and fluoride ions. In a control ^{1}H-NMR experiment, the addition of one equivalent of $(n\text{-}Bu_4N^+)OH^-$ to a solution of **L** (DMSO-D_6) showed the broadening and disappearance of the urea $-NH_{\alpha,\beta}$ signals, similar to the spectrum of **L** (DMSO-D_6) added to one equivalent of $(n\text{-}Bu_4N^+)F^-$ (Fig. S66 and S67, ESI†). The disappearance of the urea $-NH_{\alpha,\beta}$ signals upon addition of $(n\text{-}Bu_4N^+)OH^-$ and $(n\text{-}Bu_4N^+)F^-$ might suggest the deprotonation of the urea –NH proton or hydrogen bond-induced rapid dynamic effects which lead to significant –NH peak broadening. In order to validate this, the UV-vis spectra of **L** were analysed in the presence of three equivalents of $(n\text{-}Bu_4N^+)OH^-$ and $(n\text{-}Bu_4N^+)F^-$ in DMSO (Fig. 5). The UV-vis spectrum of **L** (1×10^5 mol L^{-1}) showed two absorption bands (282 nm and 355 nm); both experienced a blue shift (12 nm and 22 nm, respectively), with substantial attenuation and enhancement of the respective absorption bands, upon addition of three equivalents of $(n\text{-}Bu_4N^+)OH^-$. Furthermore, the emergence of a new band at 465 nm was also observed with a concomitant change in the color of the solution from light yellow to orange. The new band observed at 465 nm can be attributed to the deprotonation of the urea –NH proton(s), and a similar hydroxide-induced deprotonation of the urea group attached to an electron-withdrawing aromatic moiety is well documented in the literature.[16] However, the successive addition of water (up to 1 mL) to the DMSO solution mixture of **L** and $(n\text{-}Bu_4N^+)OH^-$ showed gradual attenuation of the absorption band at 465 nm (Fig. 5 inset) and the color of the solution reverted back to yellow. Thus, the control experiments proved that in a typical extraction experiment, the addition of three equivalents of $(n\text{-}Bu_4N^+)OH^-$ to a suspension of **L** in DCM leads to solubilization with concomitant deprotonation of the receptor, and the addition of an aqueous solution of Na_2HAsO_4 resulted in the protonation of the deprotonated receptor with concomitant extraction of the oxoanion in the organic phase upon continuous stirring for half an hour. The changes in the color of the organic phase observed during the entire process of arsenate extraction are also in agreement with the UV-vis spectrophotometric results (Fig. S69, ESI†).

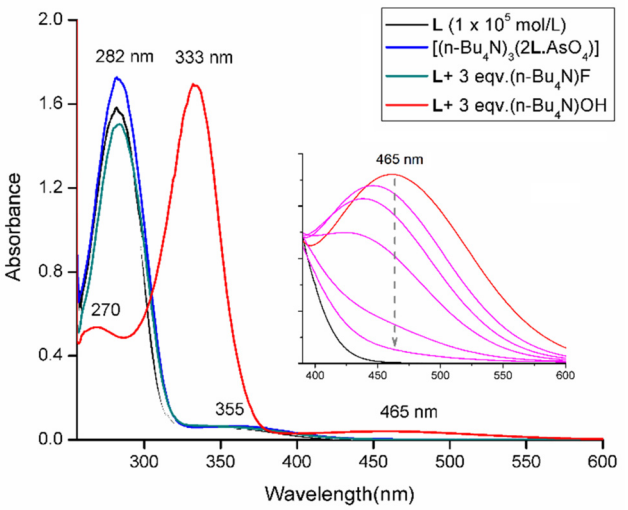

Fig. 5 UV-vis spectra of **L** and arsenate complex $[(n\text{-}Bu_4N)_3(2\mathbf{L}\cdot AsO_4)]$ in DMSO (1×10^5 mol L^{-1}) and changes in the UV-vis spectrum of **L** (1×10^5 mol L^{-1}) upon addition of three equivalents of $(n\text{-}Bu_4N^+)F^-$ and $(n\text{-}Bu_4N^+)OH^-$ in DMSO, and the inset shows the gradual attenuation of the absorption band at 465 nm of a DMSO solution mixture of **L** and $(n\text{-}Bu_4N^+)OH^-$ upon incremental addition of water up to 1 mL.

Unlike the spectral changes observed in the presence of $(n\text{-}Bu_4N^+)OH^-$, the addition of three equivalents of $(n\text{-}Bu_4N^+)F^-$ to a solution of **L** (1×10^5 mol L^{-1}) did not show any significant spectral changes, suggesting hydrogen bond-induced $-NH_{\alpha,\beta}$ peak broadening in the ^{1}H-NMR spectrum of **L** with $(n\text{-}Bu_4N^+)F^-$. The absorption band of **L** at 355 nm experienced a red shift of 15 nm in the presence of three equivalents of $(n\text{-}Bu_4N^+)F^-$ (Fig. S70, ESI†), which could possibly be the consequence of strong hydrogen bonds. However, similar shifts have not been observed in the UV-vis spectra of the arsenate and phosphate complexes in DMSO (Fig. S71, ESI†). Thus,

receptor–oxoanion complementarity plays an important role in the selective recognition of arsenate in the presence of competitive anions (hydroxides/halides/oxoanions).

Conclusion

In conclusion, we have synthesized a *N*-bridged HBD tripodal receptor for the selective extraction of arsenate from highly competitive aqueous media by encapsulation of the tetrahedral oxoanion in a π-stacked rigidified capsular assembly of the receptor by eleven strong hydrogen bonds. This is the first crystallographic evidence of the selective recognition of a pentavalent arsenate trianion (AsO_4^{3-}) by a HBD anion receptor, to the best of our knowledge. The selectivity of the receptor for AsO_4^{3-} was established by performing liquid–liquid extraction experiments, where AsO_4^{3-} can easily be extracted into the dichloromethane layer by **L** from an aqueous solution of Na_2HAsO_4 in the presence of competitive anions. DFT calculations also confirmed that the receptor has the highest binding affinity for AsO_4^{3-} when compared to other competitive oxoanions such as, PO_4^{3-}, SO_4^{2-}, CO_3^{2-} and NO_3^-.

It is important to note that the arsenate extraction experiments were carried out in the presence of a stoichiometric amount of competitive anions (halides and oxoanions), and the arsenate selectivity of the receptor may be compromised in real samples where the concentration of other anions (particularly phosphate) will be significantly higher than that of arsenate.[17]

Conflicts of interest

There are no conflicts to declare.

Acknowledgements

SKD acknowledges the Department of Science and Technology (DST) under the Ministry of Science and Technology, New Delhi for providing the research grant through an INSPIRE Faculty award (DST/INSPIRE/04/2016/001867). We also acknowledge the Director of CSIR-NEIST, Jorhat for providing access to laboratory and sophisticated analytical instrumentation facilities.

Notes and references

‡Single crystal X-ray crystallography data of $[(n\text{-}Bu_4N)_3(2\mathbf{L}\cdot AsO_4)]$ CCDC no. 2172773,† formula = $C_{144}H_{198}AsN_{29}O_{28}$, M = 2858.23, T = 120 K, space group = $P\bar{1}$, a = 17.5033(13) Å, b = 17.7141(13) Å, c = 29.548(2) Å, α = 87.526(4)°, β = 84.116(4)°, γ = 82.468(4)°, V = 9030.5(11) Å^3, Z = 2, μ = 0.254 mm^{-1}, D = 1.051 g cm^{-3}, $F(000)$ = 3044, θ(max) = 25.403, total reflections = 122 362, unique reflections = 32 853, observed reflections ($I > 2\sigma(I)$) = 25 931, parameters = 1842, $R_1(F)$ = 0.0964, w$R_2(F^2)$ = 0.2752, S = 1.068.

1 (*a*) P. L. Smedley and D. G. Kinniburgh, *Appl. Geochem.*, 2002, **17**, 517–568; (*b*) D. K. Nordstrom, *Science*, 2002, **296**, 2143–2145.

2 (*a*) WHO, *WHO Guidelines for Drinking-Water Quality*, 2nd edn, 1993 ; (*b*) M. F. Naujokas, B. Anderson, H. Ahsan, H. V. Aposhian, J. H. Graziano and W. A. Suk, *Environ. Health Perspect.*, 2013, **121**, 295–302.

3 (*a*) A. H. Smith, P. A. Lopipero, M. N. Bates and C. M. Steinmaus, *Science*, 2002, **296**, 2145–2146; (*b*) A. H. Hall, *Toxicol. Lett.*, 2002, **128**, 69–72.

4 (*a*) S. K. Acharyya, P. Chakraborty, S. Lahiri, B. C. Raymahashay, S. Guha and A. Bhowmik, *Nature*, 1999, **401**, 545; (*b*) M. L. Polizzotto, B. D. Kocar, S. G. Benner, M. Sampson and S. Fendorf, *Nature*, 2008, **454**, 505–509.

5 (*a*) W. R. Cullen and K. J. Reimer, *Arsenic is Everywhere: Cause for Concern*, RSC, 2017, pp. 266–293; (*b*) S. J. S. Flora and V. Pachauri, *Int. J. Environ. Res. Public Health*, 2010, **7**, 2745–2788; (*c*) M. J. Kosnett, *J. Med. Toxicol.*, 2013, **9**, 347–354.

6 (*a*) P. A. Gale, N. Busschaert, C. J. E. Haynes, L. E. Karagiannidis and I. L. Kirby, *Chem. Soc. Rev.*, 2014, **43**, 205–241; (*b*) S. Peng, Q. He, G. I. V. Zúñiga, L. Qin, I. Hwang, S. K. Kim, N. J. Heo, C.-H. Lee, R. Dutta and J. L. Sessler, *Chem. Soc. Rev.*, 2020, **49**, 865–907; (*c*) S. A. Boer, E. M. Foyle, C. M. Thomas and N. G. White, *Chem. Soc. Rev.*, 2019, **48**, 2596–2614; (*d*) J. Cai and J. L. Sessler, *Chem. Soc. Rev.*, 2014, **43**, 6198–6213; (*e*) S. Kubik, *Acc. Chem. Res.*, 2017, **50**, 2870–2878; (*f*) V. Amendola, D. Esteban-Gómez, L. Fabbrizzi and M. Licchelli, *Acc. Chem. Res.*, 2006, **39**, 343–353; (*g*) L. Escobar and P. Ballester, *Chem. Rev.*, 2021, **121**, 2445–2514; (*h*) L. Qin, A. Hartley, P. Turner, R. B. P. Elmes and K. A. Jolliffe, *Chem. Sci.*, 2016, **7**, 4563–4572; (*i*) L. E. Karagiannidis, C. J. E. Haynes, K. J. Holder, I. L. Kirby, S. J. Moore, N. J. Wells and P. A. Gale, *Chem. Commun.*, 2014, **50**, 12050–12053; (*j*) M. Olivari, R. Montis, S. N. Berry, L. E. Karagiannidis, S. J. Coles, P. N. Horton, L. K. Mapp, P. A. Gale and C. Caltagirone, *Dalton Trans.*, 2016, **45**, 11892–11897; (*k*) U. Manna and G. Das, *New J. Chem.*, 2018, **42**, 19164–19177.

7 (*a*) R. Dutta, P. Bose and P. Ghosh, *Dalton Trans.*, 2013, **42**, 11371–11374; (*b*) S. I. Etkind, D. A. V. Griend and T. M. Swager, *J. Org. Chem.*, 2020, **85**, 10050–10061; (*c*) M. Bayrakci and S. Yigiter, *Tetrahedron*, 2013, **69**, 3218–3224; (*d*) M. Bayrakci, S. Ertul and M. Yilmaz, *Tetrahedron*, 2009, **65**, 7963–7968.

8 (*a*) I. Ravikumar and P. Ghosh, *Chem. Soc. Rev.*, 2012, **41**, 3077–3098; (*b*) C. Bazzicalupi, A. Bencini and V. Lippolis, *Chem. Soc. Rev.*, 2010, **39**, 3709–3728; (*c*) N. Busschaert, C. Caltagirone, W. V. Rossom and P. A. Gale, *Chem. Rev.*, 2015, **115**, 8038–8155; (*d*) N. Busschaert, M. Wenzel, M. E. Light, P. Iglesias-Hernández, R. Pérez-Tomás and P. A. Gale, *J. Am. Chem. Soc.*, 2011, **133**, 14136–14148; (*e*) S. K. Dey, Archana, S. Pereira, S. S. Harmalkar, S. N. Mhaldar, V. V. Gobre and C. Janiak, *CrystEngComm*, 2020, **22**, 6152–6160; (*f*) P. A. Gale, J. R. Hiscock, C. Z. Jie, M. B. Hursthouse and M. E. Light, *Chem. Sci.*, 2010, **1**, 215–220; (*g*) J. Cai, B. P. Hay, N. J. Young, X. Yang and J. L. Sessler, *Chem. Sci.*, 2013, **4**, 1560–1567; (*h*) C. Jia, B. Wu, S. Li, X. Huang and X.-J. Yang, *Org. Lett.*, 2010, **12**, 5612–5615; (*i*) S. K. Kim, J. Lee, N. J. Williams, V. M. Lynch, B. P. Hay, B. A. Moyer and J. L. Sessler, *J. Am. Chem. Soc.*,

2014, **136**, 15079–15085; (*j*) Z. Huang, C. Jia, B. Wu, S. Jansone-Popova, C. A. Seipp and R. Custelcean, *Chem. Commun.*, 2019, **55**, 1714–1717.

9 (*a*) R. Dutta and P. Ghosh, *Chem. Commun.*, 2014, **50**, 10538–10554; (*b*) D. Yang, J. Zhao, X.-J. Yang and B. Wu, *Org. Chem. Front.*, 2018, **5**, 662–690; (*c*) C. Jia, W. Zuo, D. Zhang, X.-J. Yang and B. Wu, *Chem. Commun.*, 2016, **52**, 9614–9627; (*d*) R. Custelcean, A. Bock and B. A. Moyer, *J. Am. Chem. Soc.*, 2010, **132**, 7177–7185; (*e*) A. Rajbanshi, B. A. Moyer and R. Custelcean, *Cryst. Growth Des.*, 2011, **11**, 2702–2706.

10 (*a*) S. K. Dey, R. Chutia and G. Das, *Inorg. Chem.*, 2012, **51**, 1727–1738; (*b*) S. K. Dey and G. Das, *Dalton Trans.*, 2012, **41**, 8960–8972.

11 Tetraalkylammonium (n-Bu_4N^+/Et_4N^+) salts of arsenate/hydrogenarsenate are not available from any of the known commercial sources to the best of our knowledge.

12 Sodium hydrogenphosphate (Na_2HPO_4) and sodium phosphate (Na_3PO_4) salts are not soluble in DMSO-D_6/D_2O (9 : 1, v/v) solvent system.

13 (*a*) B. Akhuli, I. Ravikumar and P. Ghosh, *Chem. Sci.*, 2012, **3**, 1522–1530; (*b*) R. Chutia, S. K. Dey and G. Das, *Cryst. Growth Des.*, 2015, **15**, 4993–5001; (*c*) P. S. Lakshminarayanan, I. Ravikumar, E. Suresh and P. Ghosh, *Chem. Commun.*, 2007, 5214–5216.

14 M. Valiev, E. J. Bylaska, N. Govind, K. Kowalski, T. P. Straatsma, H. J. J. Van Dam, D. Wang, J. Nieplocha, E. Apra, T. L. Windus and W. A. de Jong, *Comput. Phys. Commun.*, 2010, **181**, 1477–1489.

15 M. Elias, A. Wellner, K. Goldin-Azulay, E. Chabriere, J. A. Vorholt, T. J. Erb and D. S. Tawfik, *Nature*, 2012, **491**, 134–137.

16 (*a*) V. Amendola, D. Esteban-Gómez, L. Fabbrizzi and M. Licchelli, *Acc. Chem. Res.*, 2006, **39**, 343–353; (*b*) R. Wang, X. Shu, Y. Fan, S. Li, Y. Jin and C. Huang, *RSC Adv.*, 2018, **8**, 39394–39407; (*c*) A. Basu, S. K. Dey and G. Das, *RSC Adv.*, 2013, **3**, 6596–6605.

17 K. Dabrowa, F. Ulatowski, D. Lichosyt and J. Jurczak, *Org. Biomol. Chem.*, 2017, **15**, 5927–5943.